

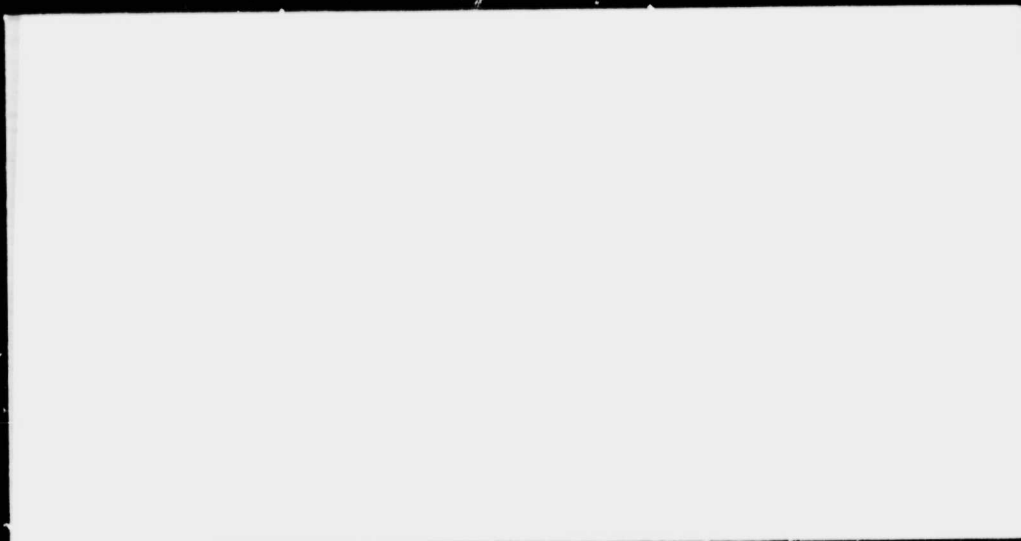
One or more of the Following Statements may affect this Document

- This document has been reproduced from the best copy furnished by the organizational source. It is being released in the interest of making available as much information as possible.
- This document may contain data, which exceeds the sheet parameters. It was furnished in this condition by the organizational source and is the best copy available.
- This document may contain tone-on-tone or color graphs, charts and/or pictures, which have been reproduced in black and white.
- This document is paginated as submitted by the original source.
- Portions of this document are not fully legible due to the historical nature of some of the material. However, it is the best reproduction available from the original submission.



FACILITY FORM 502

N 69 - 10850	
(ACCESSION NUMBER)	(THRU)
52	1
(PAGES)	(CODE)
CR-92383	28
(NASA CR OR TMX OR AD NUMBER)	(CATEGORY)



THE *M*arquardt
CORPORATION

28 OCTOBER 1968

REPORT S-899

**RESULTS OF THE PRETEST ANALYSIS OF THE
APOLLO SM-LM RCS ENGINE WHEN OPERATED
AT SEVERE OFF-LIMITS TEST CONDITIONS**

Contract No. NAS 9-7281

PREPARED BY

R.L. Moffett
R.L. Moffett, Project Engineer

APPROVED BY

D.C. Sund
D.C. Sund, Senior Project Engr.

C.A. Kerner
C.A. Kerner, Program Manager

CONTENTS

	ACKNOWLEDGEMENTS	iv
	REFERENCES	v
I	SUMMARY	1
II	INTRODUCTION	2
III	DISCUSSION	5
	A. Engine Performance at Off-Limits Conditions	6
	B. Engine Thermal Performance at Off-Limits Conditions	14
	C. Ignition at Off-Limits Conditions	30
IV	CONCLUSIONS & RECOMMENDATIONS	35
APPENDIX A	OFF DESIGN STEADY STATE AND PULSE PERFORMANCE PROGRAM	A-1

LIST OF FIGURES

<u>Figure No.</u>	<u>Description</u>	<u>Page</u>
1	Pulse Specific Impulse vs. Pulse Width at O/F = 2.0	12
2	R-4D Mixture Ratio vs. Pulse Width	13
3	Fuel Cooling Required for Preigniter Structural Safety	17
4	Preigniter Wall Heatup Time - No Film Cooling	18
5	Minimum Chamber Pressure for Safe Engine Operation	19
6	Combustor Temperature Distribution - Two Opposite Cooling Holes Plugged	26
7	Combustor Temperature Distribution - Two Adjacent Cooling Holes Plugged	27
8	Combustor Throat Circumferential Temperature Distribution	28
9	Ignition Limits	31
10	Severe Off Limits Ignition	34

LIST OF TABLES

<u>Table</u>	<u>Description</u>	<u>Page</u>
I	Severe Off Limits Test Matrix	3
II	Test Duty Cycle for Severe Off Limit Tests	4
III	Predicted Steady State Performance for Simulated Clogged Filter Test Conditions	7
IV	Predicted Pulse Performance for Simulated Clogged Filter Conditions	10
V	Development Test Runs with Low \dot{w}_1 Flow Rates	15
VI	Severe Off Limits Tests with Low \dot{w}_1 Flow Rates	16
VII	Start Up Flow For R-4D Engine at Simulated Clogged Filter Conditions	33

APPENDIX A

A-I	Computer Output-Pulse	A-2
A-II	Computer Output-Steady State	A-6
A-III	Program Listings	A-7

ACKNOWLEDGEMENTS

The author wishes to express his appreciation to J. Foote, M. Haas, J. Howell, K. Kersch, R. Reis, G. Sinclair, C. Stechman and M. Wilson for their assistance in preparing this report.

REFERENCES

1. Marquardt Test Plan (MTP) 0080 "Product Improvement Program - Severe Off-Limits Tests", September 13, 1967.
2. "Altitude Ignition of Hypergolic Bipropellant Rockets", by J.J.Kappl and R.M.Knox, 7th Liquid Propulsion Symposium, Denver, Colorado, October 1965.

I. SUMMARY

A pre-test analysis was accomplished as part of the Severe Off-Limits portion of the Product Improvement Program (NAS 9-7281), the objective being to predict the effects of failure of several Apollo RC System components upon the operation of the RCS engine. The results of this analysis will be used primarily for intelligent test planning. In addition, the results and techniques developed during this analysis will be extended for use during the Reduced Fuel Cooling and the Optimized Apollo SM-LM RCS Engine Injector portions of the Product Improvement Program.

Analyses were performed to determine the steady state and pulsing performance, to evaluate the thermal effects to the preigniter and molybdenum combustor, and to evaluate engine ignition when operating at test conditions simulating clogged propellant system filters. The results show that the tip of the preigniter may possibly be eroded on two of these system failure simulation runs. Additionally, the analyses show that at several of the test conditions simulating serious filter clogging inconsistent preigniter operation can be expected, accompanied by long ignition delays. Possible combustor damage can result from ignition overpressures that might be caused by the excessive ignition delays.

The performance and thermal analyses of the simulated clogged filter tests are also applicable for the simulated regulator failure tests. The reduced flow caused by regulator failure may lead to erosion of the preigniter tip due to insufficient fuel cooling.

Another system failure to be simulated will be plugging or clogging of the injector holes with contaminants. No engine damage is predicted for the plugged orifice tests to be conducted.

II. INTRODUCTION

The Severe Off-Limits phase of the Product Improvement Program (NAS 9-7281) consists of several off-design tests intended to determine the effects of possible Apollo SM-LM RC system component failures upon the SM-LM RCS engine (TMC designation R-4D) when operating during and/or following these failures. For these tests the system failures will be simulated (e.g., decreasing propellant supply pressure to simulate filter clogging which throttles propellant flow) instead of actually causing system component failure. The system failures to be simulated are clogged propellant filters (causing reduced flow), pressure regulator malfunction (stopping supply of propellant pressurant gas) and clogged engine injector orifices from upstream contamination. Two refurbished R-4D engines are to be used to accomplish these tests. The Severe Off-Limits test matrix is shown in Table I and II. The detailed test plan is contained in Reference 1.

A pretest analysis was performed to predict the results of the Severe Off-Limits tests upon the R-4D engine. The purpose of this analysis was twofold. First, since engine damage could occur from the severity of the off-design test conditions, the analysis results were used to plan efficient test facility utilization by sequencing the tests such that potentially damaging test conditions are separated by sufficient time to repair one engine (if it is damaged) while the other continues testing. Also the pretest analysis will provide useful techniques and experience to be used for other portions of the Product Improvement Program, notably the Reduced Film Cooling Evaluation and the Optimized SM-LM RCS Engine Injector tasks.

SEVERE OFF-LIMITS TEST MATRIX

Test Title	Engine & Propellant Temperatures	Propellant Inlet Pressures under Firing Conditions (see below)	Duty Cycle	Type of Propellants
Clogged Filter, Performance	Ambient	Group 1 Group 2 Group 3	Matrix A Table II	N_2O_4/MMH
Clogged Filter, Ignition	Minimum	Group 1 Group 2 Group 3	Matrix B Table II	$[N_2O_4/MMH]$ $[N_2O_4/A-50]$
Pressure Regulator Failure	Ambient	Decay from 170 psia to 25 psia during run	500 second run	H_2O_4/MMH
Clogged Orifice	Ambient	(a) of Group 1	Matrix A Table II	N_2O_4/MMH

PROPELLANT INLET PRESSURES (Psia)

	Group 1		Group 2		Group 3	
	Fuel	Oxidizer	Fuel	Oxidizer	Fuel	Oxidizer
(a)	170	170	170	150	150	150
(b)	150	170	*170	100	*100	100
*(c)	100	170	170	50	50	50
(d)	50	170				

*Tested with both A-50 and MMH Fuels.

TABLE I

TEST DUTY CYCLE

SEVERE OFF-LIMIT TESTS

MATRIX A - PERFORMANCE TESTS

Electrical "On" Time	Electrical "Off" Time	Number of Pulses	Number of Runs
0.020 sec.	0.480 sec.	150	1
0.050 sec.	0.450 sec.	60	1
0.100 sec.	0.100 sec.	30	1
0.500 sec.	0.100 sec.	10	1
5.0 sec.	-	1	3
50.0 sec.	-	1	1

MATRIX B - IGNITION TESTS

Electrical "On" Time	Electrical "Off" Time	Number of Pulses	Number of Runs
0.012 sec.	0.100 sec.	10	5
0.012 sec.	0.350 sec.	10	5
0.012 sec.	0.600 sec.	10	5
0.012 sec.	1.00 sec.	10	5
0.012 sec.	1.50 sec.	10	5
0.012 sec.	3.00 sec.	10	5

III. DISCUSSION

The pretest analysis consisted of the following items. The thermal and performance (steady state and pulsing) effects on the R-4D when the inlet pressures are reduced simulating clogged filters or failed pressure regulators were predicted. The thermal effects upon the preigniter and main chamber caused by plugged injector holes was also evaluated. A criterion for good ignition was developed and was used to predict the ignition behavior of the R-4D engine when tested at conditions simulating clogged propellant filters.

The starting points for all of these analyses were previous reports and test results wherever available. When existing information was incomplete or non-existent, then original analysis efforts were performed.

The results of the Severe Off-Limits pretest analyses are discussed in the following sections.

A. Engine Performance at Off-Limits Conditions

To aid in the prediction of engine performance at off design conditions an IBM Quiktran computer program was written. This program is capable of predicting both steady state and pulsing engine performance. The mathematical model, which the computer program is based on, consists mainly of fundamental rocket engine relationships involving pressure and flow characteristics. In addition, actual test data of specific impulse (Isp) as a function of mixture ratio (O/F) was made an integral part of the computer program. A listing of this program, as well as sample output, is given in Appendix A.

The steady state section of the performance computer program predicts steady state values for thrust, mixture ratio, chamber pressure and specific impulse. These results for the off limit test conditions simulating clogged propellant filters are shown in Table III.

The first step in the computer program is the calculation of engine flow coefficients and a "pseudo" thrust coefficient from R-4D engine data at nominal operating conditions. The "pseudo" thrust coefficient, is calculated from equation (1).

$$TCO = \frac{PC_{nom}}{F_{nom}} = \frac{1}{A_t C_f} \quad (1)$$

where TCO = "pseudo" thrust coefficient

PC = chamber pressure

F = thrust

A_t = engine throat area

C_f = thrust coefficient

and the subscript "nom" refers to nominal conditions.

PREDICTED STEADY STATE PERFORMANCE
FOR SIMULATED CLOGGED FILTER TEST CONDITIONS

P_{ox} (psia)	P_f (psia)	O/F	F (lb)	I_{sp}	P_c
170	170	2.030	100.00	281.5	96.5
170	150	2.351	94.7	269.9	91.4
170	100	3.823	75.1	217.3	72.5
170	50	6.853	39.9	109.2	38.5
150	170	1.748	96.1	290.9	92.7
100	170	1.064	76.1	274.6	73.5
50	170	0.539	42.4	177.3	40.9
150	150	2.030	91.5	281.0	88.3
100	100	2.030	67.9	279.7	65.6
50	50	2.030	39.6	278.0	38.2

For engines exhausting into space (or a vacuum), the real thrust coefficient, C_f , is a function of the chamber/exit pressure ratio, P_c/P_e , and the ratio of specific heats, γ , of the gaseous combustion products. In actuality γ varies slightly with chamber pressure and mixture ratio, but for the purpose of this program this variation has been neglected and TCO is assumed constant for all operating conditions. The engine flow coefficients are calculated according to equation (4) and (5) using the nominal propellant flow values calculated from equations (2) and (3).

$$WF_{nom} = \frac{F_{nom}}{(I_{sp})_{nom} (1 + O/F)} \quad (2)$$

$$WO_{nom} = (WF_{nom}) (O/F) \quad (3)$$

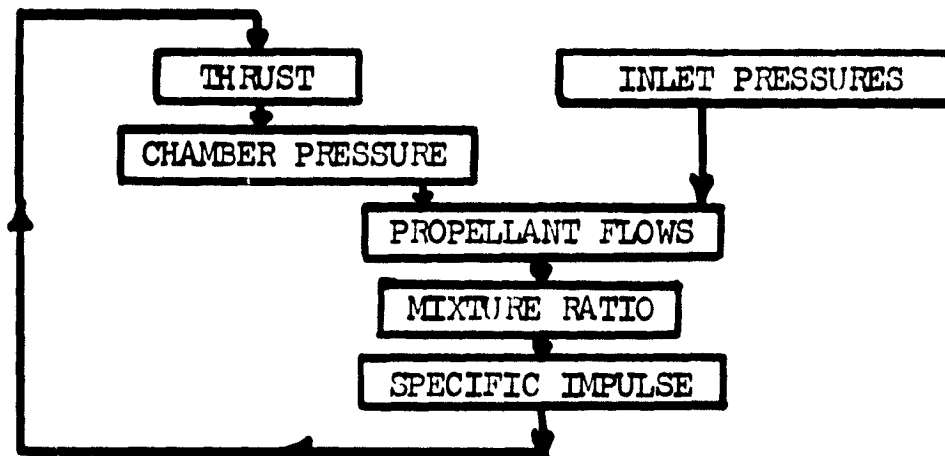
$$XKF = \frac{WF_{nom}}{(P_{tank})_{nom} - PC_{nom}} \quad (4)$$

$$XKO = \frac{WO_{nom}}{(P_{tank})_{nom} - PC_{nom}} \quad (5)$$

where

WF	=	fuel flow rate
WO	=	oxidizer flow rate
I_{sp}	=	specific impulse
O/F	=	mixture ratio
P_{tank}	=	propellant tank pressure
XKF	=	fuel flow coefficient
XKO	=	oxidizer flow coefficient

An iteration process is used to solve for performance parameters of off design operating conditions. The basic loop in this iteration process is as follows:



An arbitrary value of $F = 100$ lb. is taken as the starting point. The iteration process is complete when two successive thrust values are within .001 lb. of each other.

The pulse section of the performance computer program predicts values of specific impulse and mixture ratio. These results for the off-limit test conditions simulating clogged propellant filters are shown in Table IV.

The first step in the determination of pulsing performance is the calculation of the comparable steady state performance values as previously described. These steady state values are then multiplied by a correction factor which is discussed below.

In the case of specific impulse a mathematical expression was used to describe the correction factor. A least squares curve fitting analysis was made with existing R-4D acceptance test data to determine this mathematical expression. The expression best representing the data is given in equation (6).

$$\eta = A_1 (\text{epw}) + A_2 (\text{epw}) + A_3/\text{epw} + A_4 \quad (6)$$

where $\eta = \eta(\text{epw}) =$ specific impulse correction factor

$A_1, A_2, A_3, A_4 =$ constants

epw = electrical pulse width

PREDICTED PULSE PERFORMANCE FOR SIMULATED CLOGGED FILTER CONDITIONS

P _{ox} /P _f	PULSE WIDTH							
	20 ms		50 ms		100 ms		500 ms	
	O/F	I _{sp}	O/F	I _{sp}	O/F	I _{sp}	O/F	I _{sp}
170/170	1.76	188.5	1.94	236.7	1.99	258.0	2.02	276.6
170/150	2.01	180.7	2.24	226.9	2.30	247.3	2.34	265.1
170/100	3.16	145.1	3.60	182.1	3.72	198.5	3.81	212.8
170/50	5.46	72.6	6.35	91.1	6.61	99.3	6.81	106.5
150/170	1.55	194.9	1.69	244.7	1.72	266.7	1.74	285.9
100/170	.99	183.6	1.04	230.5	1.05	251.3	1.06	269.4
50/170	.526	118.1	.538	148.3	.538	161.6	.537	173.2
150/150	1.77	188.2	1.95	236.3	1.99	257.5	2.02	276.1
100/100	1.80	187.3	1.96	235.1	2.00	256.3	2.02	274.8
50/50	1.83	186.2	1.97	233.7	2.00	254.8	2.02	273.1

To best define this correction over the entire range of pulse widths of interest, two sets of constants (A_1, A_2, A_3, A_4) were used; one for pulse widths less than 100 ms, and one for pulse widths greater than 100 ms. The resulting curve of pulse specific impulse vs. electrical pulse width is shown in Figure 1 for the R-4D engine operating at nominal conditions.

The determination of the mixture ratios (O/F) at the off-design test conditions requires two correction factors. The product of these correction factors is multiplied times the steady state O/F to give the predicted pulse O/F. One correction factor, similar in form to equation (6), expresses the O/F as a function of the pulse width assuming the valve opening and closing times do not vary from those at nominal conditions. But since different inlet pressures will be used to simulate the flows caused by filter clogging, a second correction factor had to be incorporated to account for valve response as a function of the pressure. The curve of pulse mixture ratio vs. electrical pulse width is shown in Figure 2 for nominal operating conditions, including equal tank pressures. Two acceptance test data points are shown on this figure for comparison.

With regard to the valve opening time correction factor, a mathematical expression was generated which relates the valve opening and closing times with the pulse width and tank pressures. The resulting expression is given in equation (7).

$$K = \frac{epw - .00185 P_o + 1.15 - 17.67/epw}{epw - .00146 P_f + 2.23} \quad (7)$$

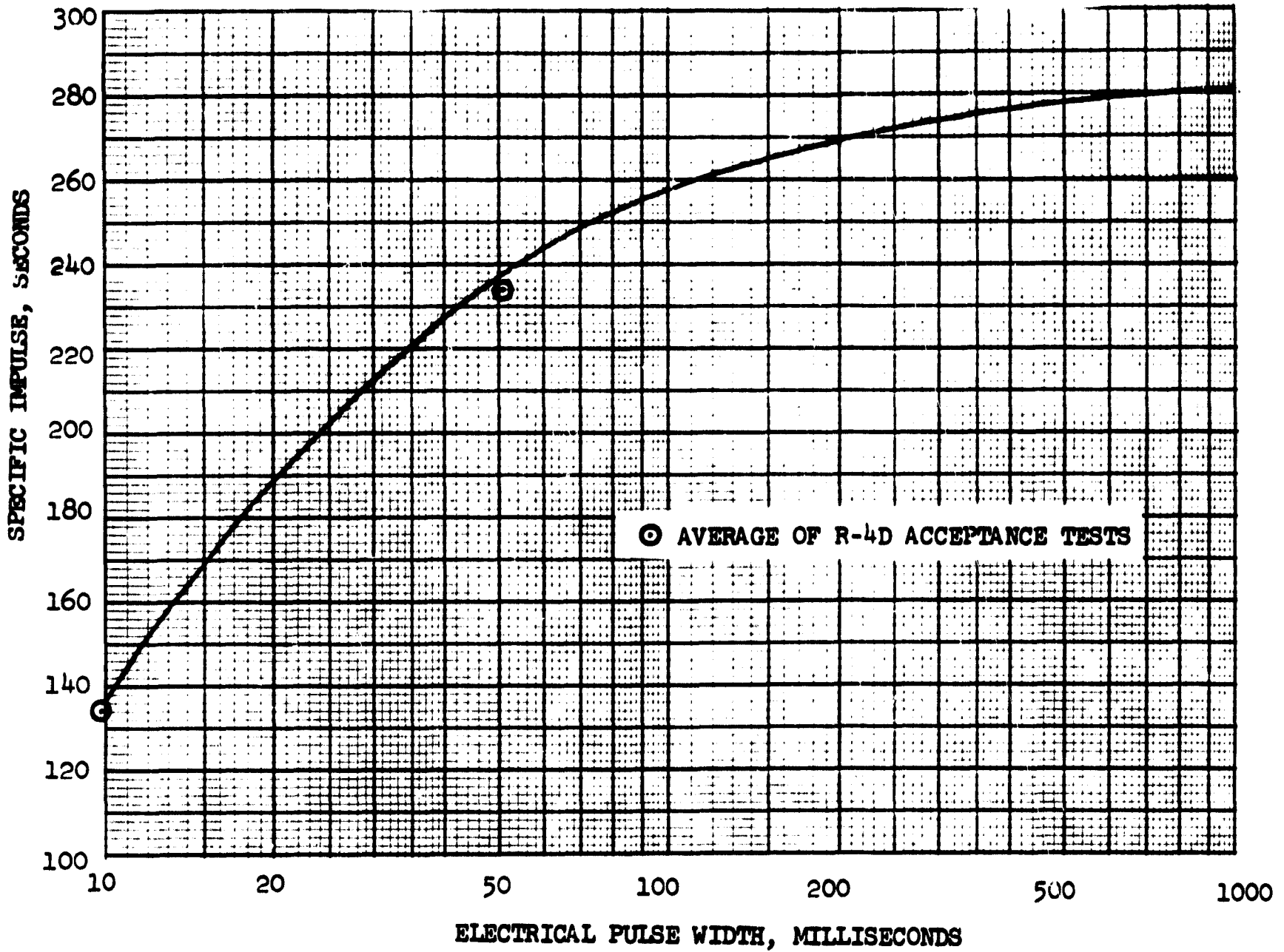
where $K = K(epw, P_o, P_f)$ = mixture ratio correction factor

P_o = Oxidizer tank pressure

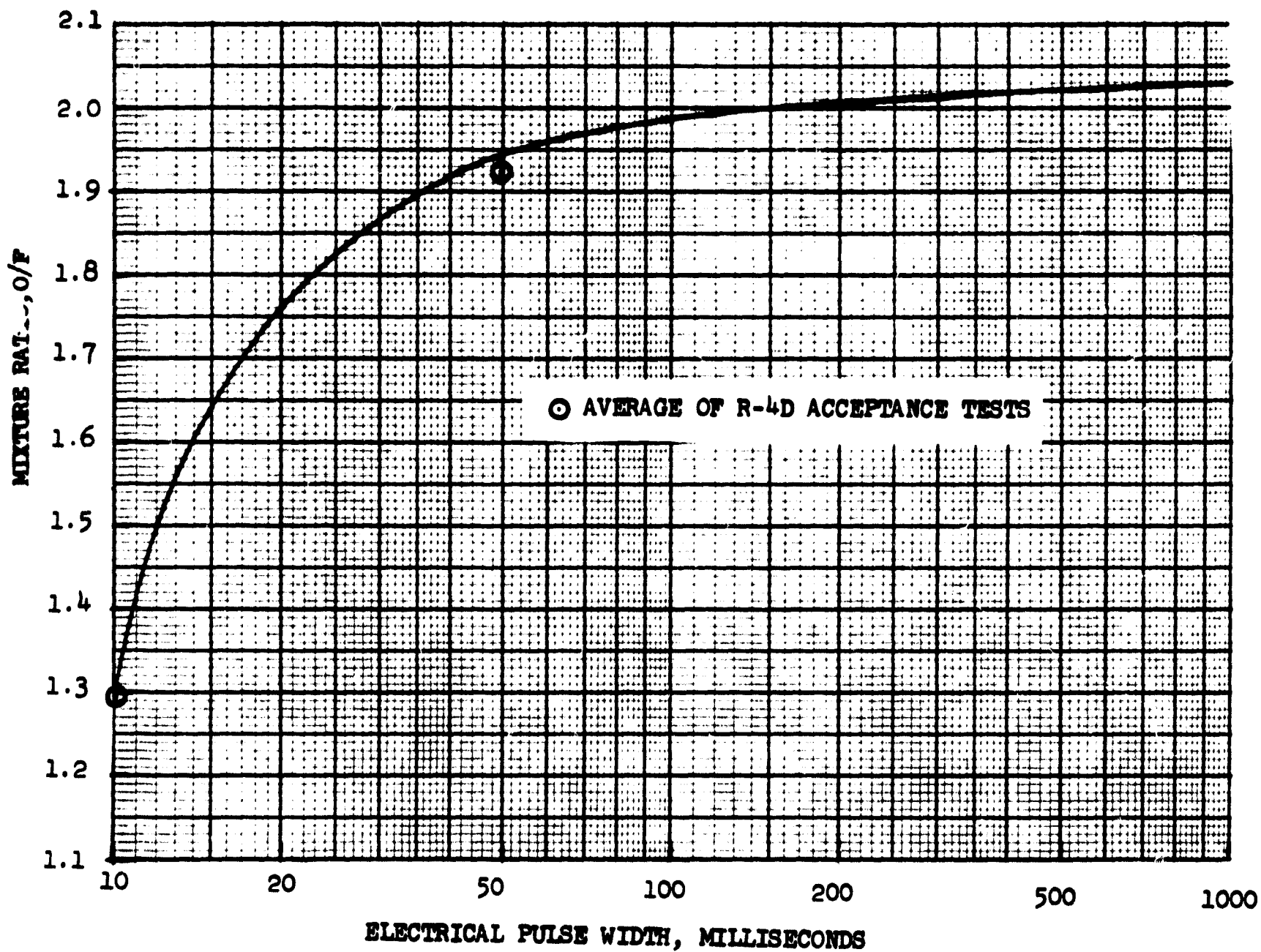
P_f = Fuel tank pressure

epw = electrical pulse width (ms)

PULSE SPECIFIC IMPULSE VS. PULSE WIDTH AT O/F = 2.0



R-4D MIXTURE RATIO VS. PULSE WIDTH



B. Engine Thermal Performance at Off-Limits Conditions

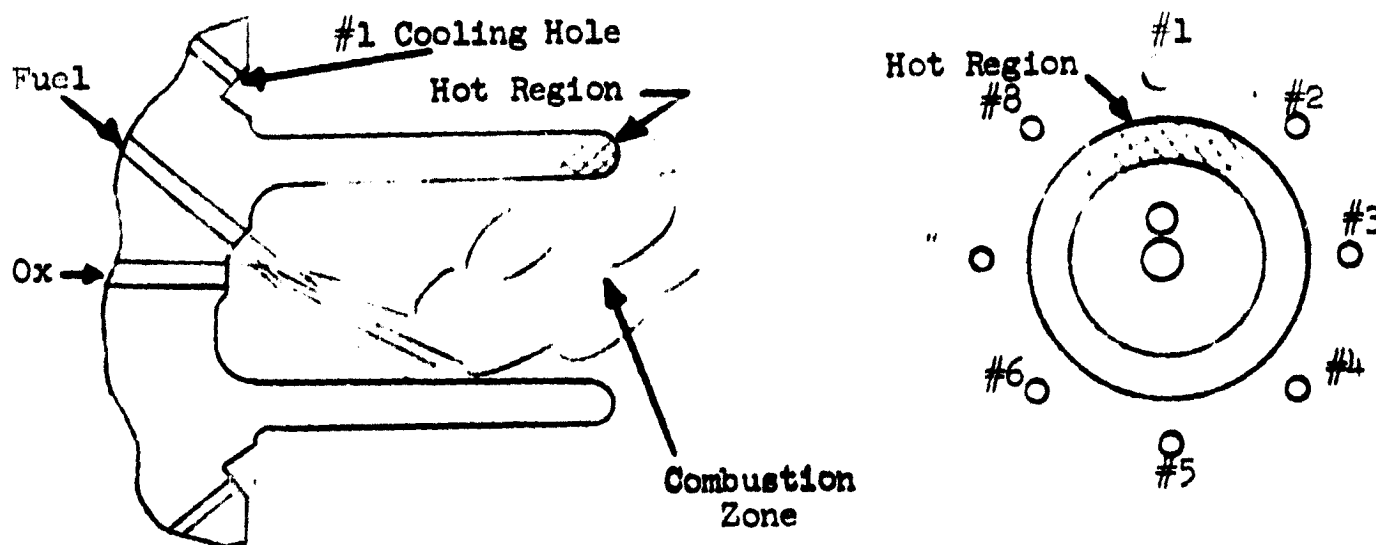
Drawing upon previous R-4D engine development experience, two modes of potential engine damage resulting from the thermal effects of off-design operational conditions were recognized and analyzed. These potential problem modes are preigniter burnout due to insufficient fuel cooling flow and combustor burnthrough also due to insufficient fuel cooling flow.

This previous development data indicates that preigniter burnout during the Severe Off-Limits tests is possible only at conditions of reduced total fuel flow (i.e., during the simulated clogged filter and simulated regulator failure tests) and at conditions of localized reduction of the preigniter cooling flow as in the clogged injector holes tests. Combustor burnthrough would be possible only during the simulated clogged orifice tests where two of the combustor cooling holes will be plugged during engine operation. Only the above mentioned conditions where thermal damage was thought possible were analyzed.

All of the previous R-4D development engine test experience has been with A-50 fuel therefore some qualification of the predicted MMH thermal results may be necessary due to the differences in thermal properties of the two fuels. Where appropriate, these differences are discussed below.

During the development stage of the R-4D engine, three early design engines suffered preigniter burnout or near burnout. These burnouts characteristically occurred at the tip of the preigniter cup on the side near the fuel valve. At the time of this burnout problem the fuel coolant flow was evenly distributed around the cup and it was reasoned that the side of the cup where the burnout occurred was hotter because it was in the path of resultant preigniter combustion gasses. The opposite side is cooler probably due to propellant splash. The picture below illustrates the suspected flow and combustion regimes at the preigniter.

R-4D Preigniter



To prevent burnout at the point of high heat flux, the flow rate out of the hole that cools this area was increased. By doubling the diameter of this hole, the flow rate over the critical area was quadrupled. This diameter change proved successful and present R-4D engines utilize this design for ensuring trouble free preigniter operation. The Marquardt hole numbering system specifies the enlarged orifice as the #1 preigniter cooling hole and this terminology will be used in subsequent discussion.

The cited test experience plus thermal analysis point to the flow out of the #1 hole (\dot{w}_1) as being the single most important parameter for determining adequate preigniter cooling. Other effects such as preigniter O/F and flow rate, main chamber combustion temperature, flow from other cooling holes, etc., are secondary. Therefore, in the analysis of preigniter burnout, flow from the #1 cooling hole was used as the determining criteria.

Many of the simulated clogged filter test conditions will have less than nominal #1 cooling flow due to either throttled fuel flow alone or due to both propellants being reduced. Since the fuel distributional flow remains relatively constant at all flow rates, a reduction in total fuel flow rate results in a nearly proportionate reduction in #1 cooling flow. Table V contains a listing of previous test experience where runs with reduced total fuel flow were conducted. All of these engines had normal hole sizes. Preigniter burnout occurred during one firing. Injector head water flow testing of this engine subsequent to the failure showed that the flow out of the #1 cooling hole was only 85% of the minimum acceptable flow standard. This engine incurred preigniter burnout on a run conducted at 79 psia chamber pressure (about 81 pounds thrust or 81% of nominal flow). Therefore, the flow through the #1 hole during the failure run was only about 69% of minimum expected flow. The preigniter burnout on this engine test proves valuable in this analysis since it can be used to help define the lower limit of #1 cooling flow where burnout becomes probable.

TABLE V

DEVELOPMENT TEST RUNS WITH LOW \dot{w}_1 FLOW RATES

No. Key for Figure 3	Engine	Duration	\dot{w}_1 (lb/sec)	O/F	P_c (psia)
1*	10670, S/N 2-1	34 sec	3.84×10^{-3}	1.98	79
2	10670, S/N 2-1	60	4.6	2.12	96.5
3	10670, S/N 2-1	80	4.6	1.96	92.5
4	10670, S/N 1-7	5	3.38	2.2	62
5	10650, S/N 2-10	80	5.25	2.18	98
6	12340, S/N 1-18	51	4.18		
7	228687, S/N 13	60	5.78	1.74	85.5
8	228687, S/N 13	60	5.5	1.93	91.5

*Preigniter burned out at the tip of the cup nearest the fuel valve near the end of the run.

The #1 cooling flows (\dot{w}_1) on the runs shown on Table V are plotted on Figure 3 vs. burntime. A horizontal line at $\dot{w}_1 = 4 \times 10^{-3}$ pps indicates approximate level of cooling flow, as suggested by the plotted data, below which or near which preigniter burnout is probable. One of the previous development test runs (No. 4 on Table V) was at a \dot{w}_1 less than 4×10^{-3} but the run duration was only 5 seconds and probably not long enough for steady state temperatures to be reached on the preigniter. A simple heat transfer analysis, assuming a preigniter gas temperature of 3000°F and no fuel cooling or radiation cooling of the cup showed that the melting point of the material is just reached at 5 seconds under such severe conditions (see Figure 4). The burnout region on Figure 3 is further restricted by eliminating runs of 5 seconds or less in duration.

The predicted performance parameters (from Section A) and #1 coolant flow rates during the simulated clogged filter runs that will have reduced cooling flow are shown on Table VI and are plotted on Figure 3. Since burnout is more probable on long runs, only the 50 second run of the duty cycle is listed. Figure 3 indicates that preigniter burnout may occur on the test runs listed in Table VI as run Nos. 10, 11, 13 and 14.

TABLE VI

SEVERE OFF-LIMITS TESTS WITH LOW \dot{w}_1 FLOW RATES

No Key for Figure 3	Oxidizer Inlet Pressure (psia)	Fuel Inlet Pressure (psia)	Duration	\dot{w}_1 (lb/sec)	O/F	P_c (psia)
9	170	150	50	4.93	2.35	91.4
10	170	100	50	3.37	3.82	72.5
11	170	50	50	2.20	6.85	38.5
12	150	150	50	5.06	2.03	88.2
13	100	100	50	3.54	2.03	65.6
14	50	50	50	2.20	2.03	38.2

The burnout region is further defined as a function of chamber pressure and O/F as shown in Figure 5. The line defining the probable burnout region was determined from:

$$\dot{w}_1 = \frac{k P_c}{97 I_{sp} (1 + O/F)}$$

FUEL COOLING REQUIRED FOR PREIGNITER STRUCTURAL SAFETY

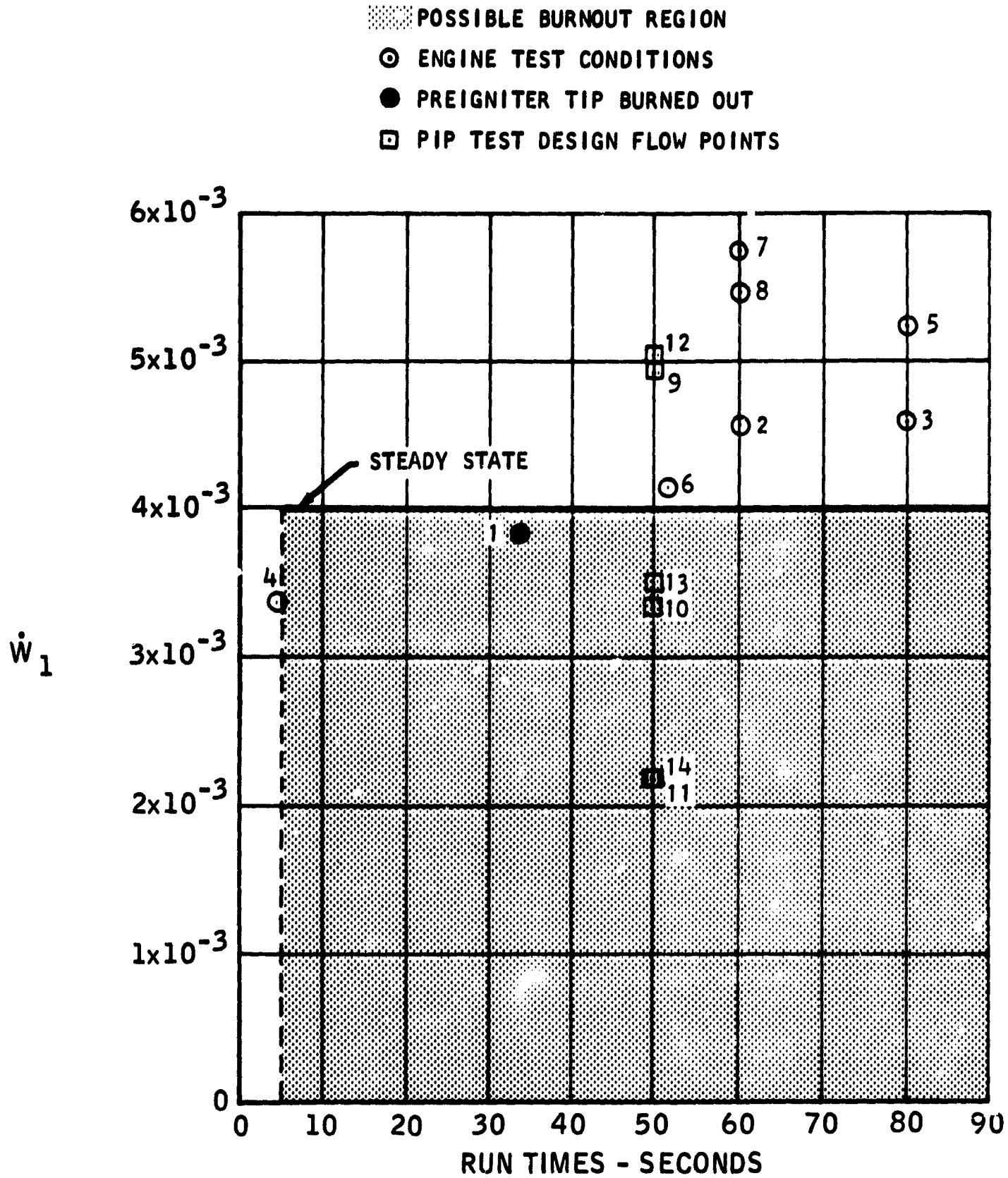
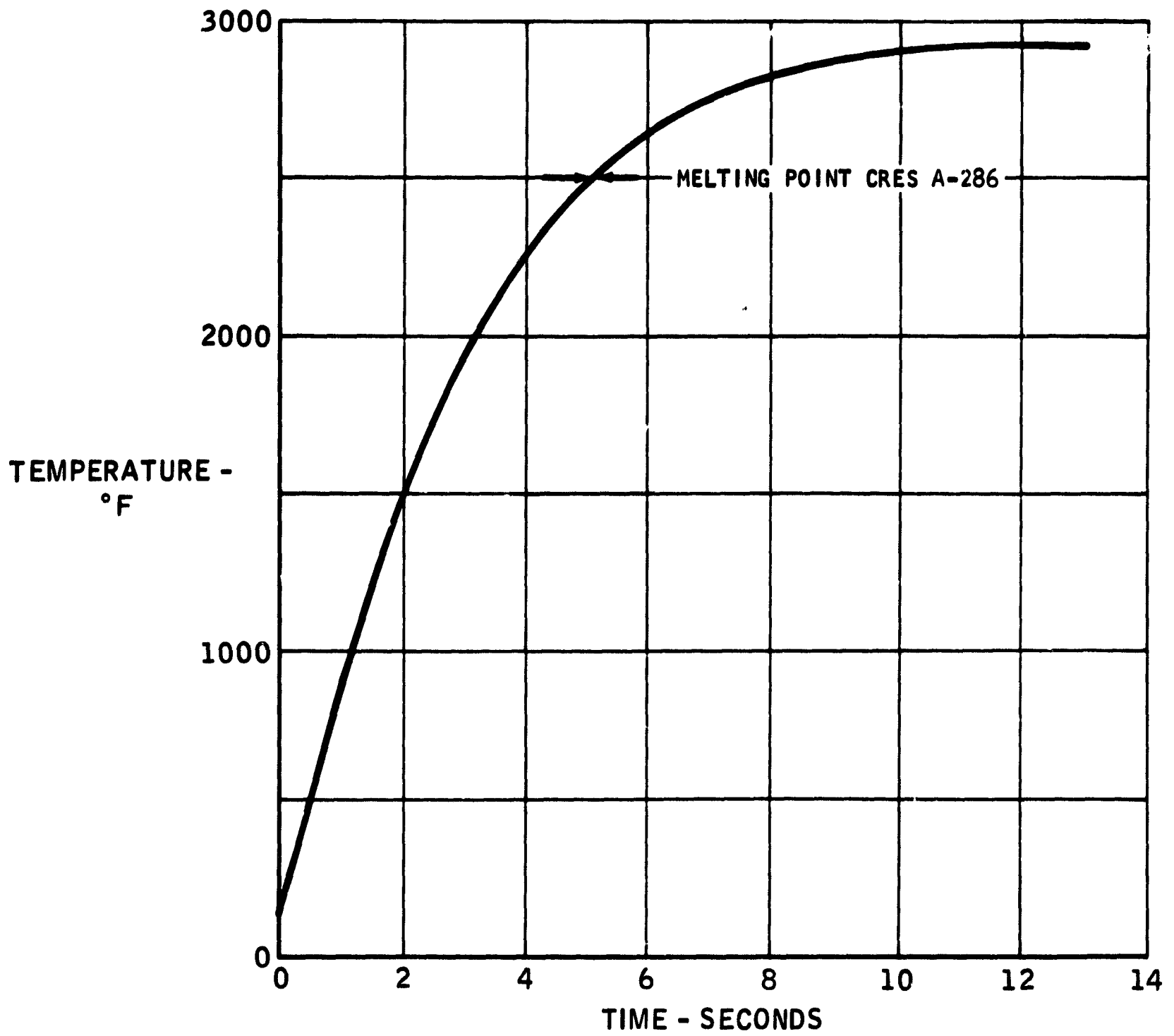


FIGURE 3

PREIGNITER WALL HEATUP TIME NO FILM COOLING



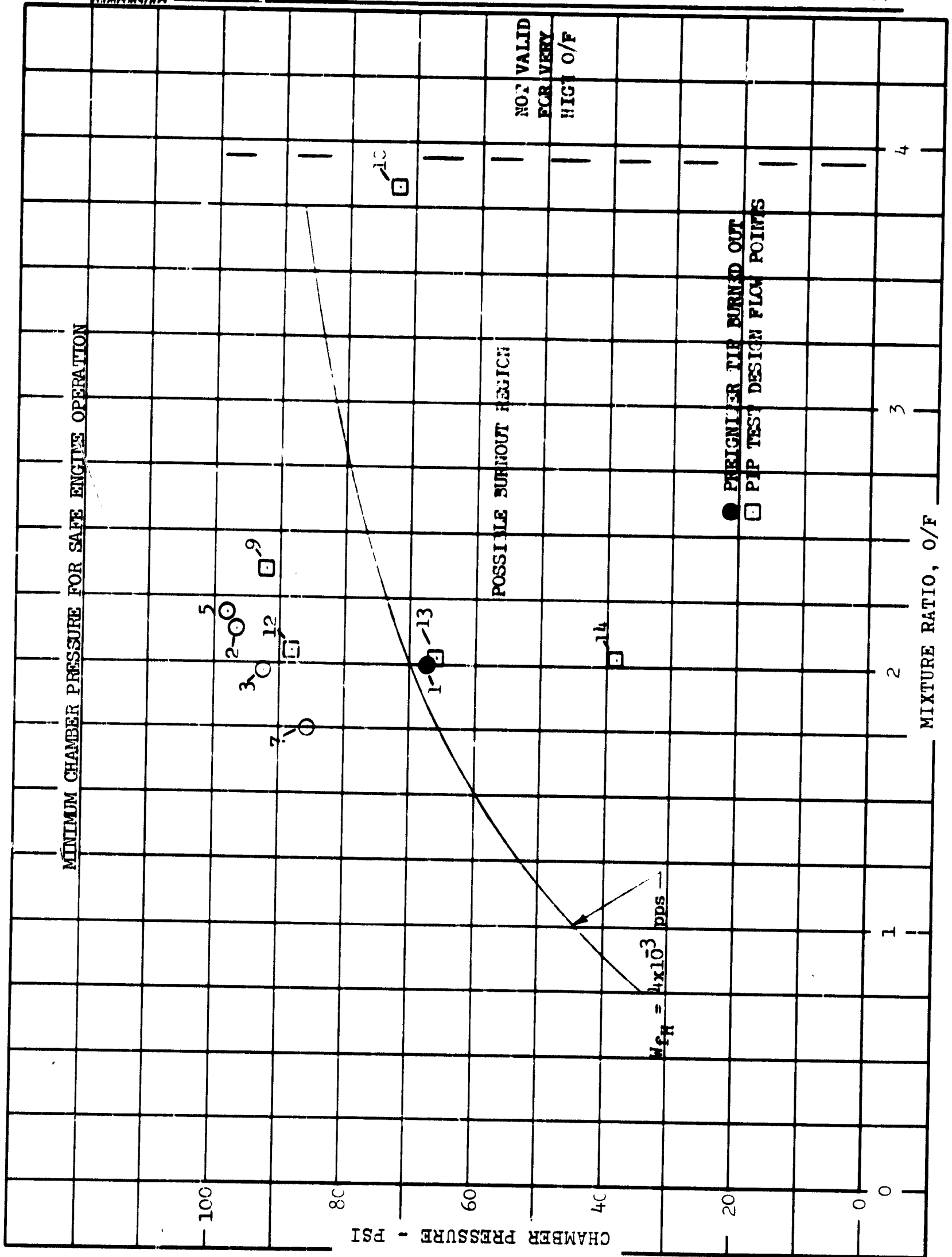


FIGURE 5

where: $\dot{w}_1 = 4 \times 10^{-3}$ pps
 k = percent of nominal total fuel flow represented by \dot{w}_1
 P_c = chamber pressure
 I_{sp} = specific impulse at O/F
 O/F = propellant mixture ratio

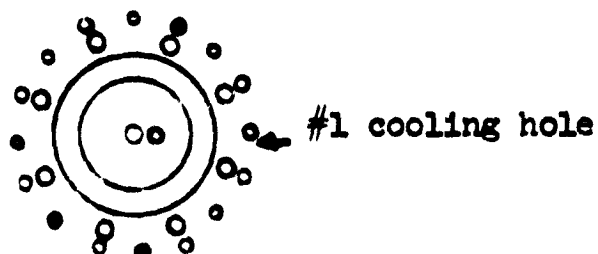
The burnout region on Figure 5 considers O/F and P_c to affect preigniter burnout only when these conditions cause the #1 cooling flow (\dot{w}_1) to drop to below the adequate value. The burnout run (No. 1 on Table V) is plotted at 67 psia to reflect the pressure that would accompany a normal engine where the #1 cooling flow would be equal to the \dot{w}_1 measured on the burnout engine (i.e., 85% of the measured P_c value of 79 psia).

The same four simulated clogged filter runs that may burn out as indicated by Figure 3 may also burn out per Figure 5 except that the burnout region on Figure 5 is limited to O/F below 4.0 to account for low efficiency combustion at high O/F. Combustion temperature past the cutoff region is probably less than 50% of that at an O/F of 2.0. Therefore, No. 11 (Table VI) is eliminated as a possible burnout run and No. 10 is questionable. PIP runs 13 and 14 are the only runs that may therefore experience preigniter failure.

The simulated regulator failure test was not dynamically analyzed for preigniter burnout. However, the clogged filter conditions (equal pressures) analyzed represent points on the pressure decay curve during the simulated regulator failure test. Since the pressures pass through the point conditions, burnout would not be expected at the upper limit conditions predicted in the previous analysis since some length of burn time is required to reach the burnout temperature. During the simulated regulator failure run the engine may enter the burnout region shown in Figures 3 and 5 and proceed well into the region before burnout is experienced. Preigniter burnout may occur, however, prior to the inlet pressures reaching the conditions of Run No. 14 on Figure 5 (50 psia oxidizer and fuel inlet pressure).

The possibility of encountering preigniter burnout during the plugged injector orifice testing was analyzed. One of the two plugged hole configurations requires plugging two preigniter cooling holes and a fuel doublet hole as shown in the following figure. The outer ring of holes are fuel doublet and preigniter cooling holes, and the inner ring is oxidizer doublet holes.

Preigniter Cup Viewed From The Throat

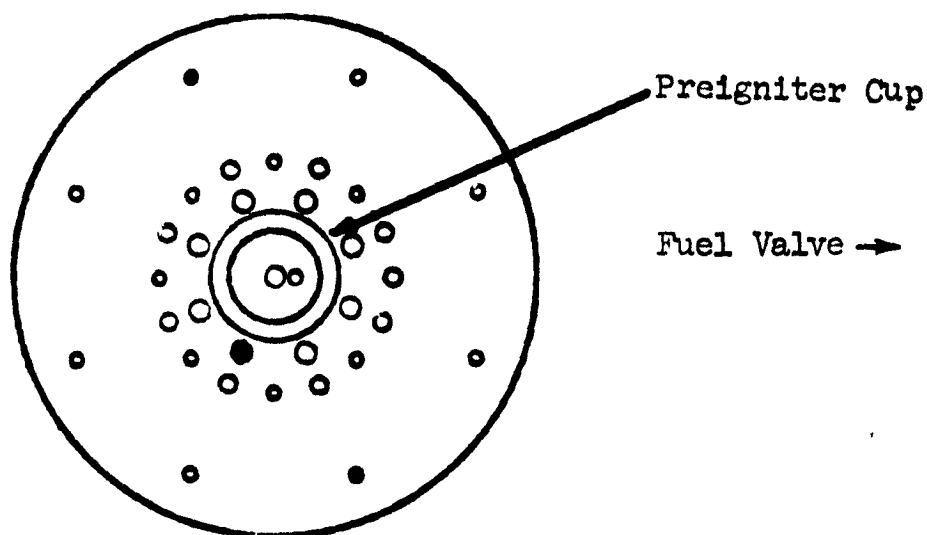


• indicates holes to be plugged.

Since the previous preigniter burnout analysis considered only the flow from the #1 cooling holes as the only controlling factor, this model obviously cannot be used for this plugged orifice configuration. Experience would suggest that this configuration would not experience preigniter burnout during engine operation. The holes to be blocked cool the cooler areas of the cup and sufficient cooling would be provided from the immediately adjacent holes. Also, since the fuel doublet hole opposite the two plugged cooling holes will be plugged, there will be no flux from this doublet.

The molybdenum combustor of the R-4D engine is cooled partially by radiation and partially with a fuel film. The film cooling is applied by impinging eight evenly spaced fuel streams upon the combustor wall near the injector-combustor attach flange. During the conduct of the test with plugged injector orifices, one of the two configurations will have two of the combustor cooling holes plugged and a oxidizer doublet plugged. The following figure illustrates the holes to be plugged.

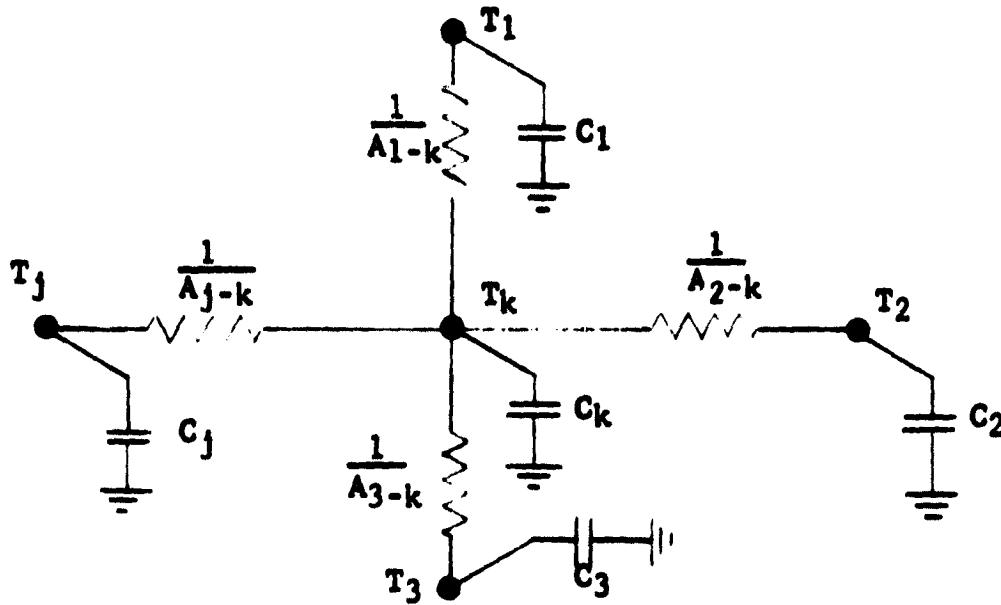
Injector Face As Viewed From The Throat



Solid holes represent plugged holes.

Since the two opposite plugged combustor cooling holes chosen are not unique, the more general case of plugging any pair of opposite cooling holes was analyzed. Also, since a computer program was used for the analysis, the more severe condition of plugging two adjacent cooling holes was evaluated also.

The thermal analysis was performed using the thermal analyzer computer program. This program solves the appropriate heat transfer equations at each specified location (node) in the engine by a finite difference technique. The procedure can be visualized by using an analogy between heat transfer and electrical circuits.



Typical Heat Transfer Network Electrical Analogy

From an energy balance at each node

$$C \frac{dT}{d\theta} = \sum_{j=1}^n T_j A_{j-k} - T_k \sum_{j=1}^n A_{j-k}$$

or in finite difference notation

$$\frac{T(\theta + \Delta\theta) - T_\theta}{\Delta\theta} = \frac{1}{C} \left\{ \sum_{j=1}^n T_j A_{j-k} - T_k \sum_{j=1}^n A_{j-k} \right\}$$

where C = thermal capacity of specified lump or node

θ = time

T_θ = initial temperature at time θ ($^{\circ}\text{F}$)

$T(\theta + \Delta\theta)$ = temperature after time interval $\Delta\theta$

A_{j-k} reciprocal of thermal resistance for conduction, convection, or radiation between nodes

Heat transfer coefficients for the combustion gases were obtained using the modified Bartz equation which follows:

$$h_{cg} = \frac{0.026}{D^{*.2}} \frac{\mu_f^{.2}}{Pr_f^{.6}} \left(\frac{W}{A^*}\right)^{.8} \left(\frac{A^*}{A}\right)^{.9} \left(\frac{H_R - H_w}{T_R - T_w}\right)^\sigma$$

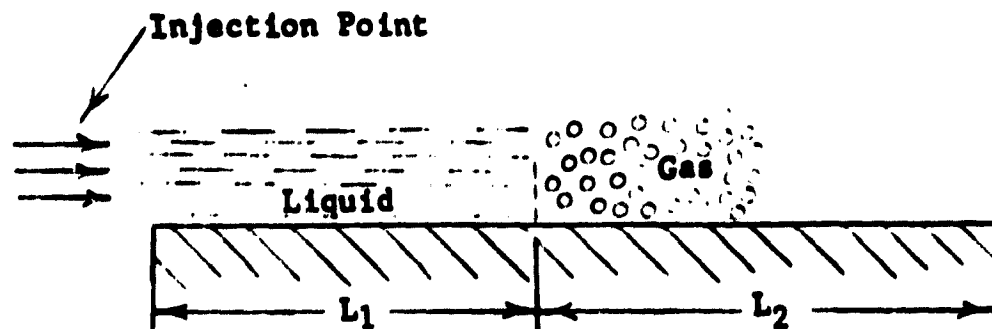
where h_{cg} = heat transfer coefficient
 D = diameter
 Pr = Prandtl number
 μ = viscosity
 w = propellant flow rate
 A = flow area
 σ = correction factor
 H = enthalpy of gas
 T = temperature

subscripts

* = throat conditions
 f = film temperatures
 R = recovery temperature
 w = wall temperature

The heat transfer from the combustion gases to the chamber and nozzle depends upon the heat transfer coefficient and also upon the gas temperature at the edge of the boundary layer. These temperatures have been predicted using the Marquardt Film Cooling Computer Program

The chamber and nozzle is film cooled by the fuel which is injected along the walls of the chamber. The liquid layer cools a major portion of the chamber and the gaseous film cools the convergent section of the nozzle. The evaporative film cooling correlations have been derived for the simplified physical model shown below:



The equation for the length of the liquid portion of the film coolant is:

$$L_1 = C \left[\frac{W_{fc} C_{pL} (T_v - T_i)}{Ph_{cg} (T_R - T_v)} + \frac{W_{fc} \Delta H_v}{Ph_{cg} (T_R - T_v)} \right]$$

where:

- C = mixing constant (1.0 - 1.5)
- W_{fc} = weight flow of coolant
- C_{pL} = Specific heat of coolant
- T = temperature
- P = chamber perimeter
- h_{cg} = heat transfer coefficient
- ΔH_v = heat of vaporization

Subscripts:

- v = vapor
- R = recovery
- i = initial

At L_1 , the liquid film coolant is vaporized and is assumed to be saturated vapor. The equations used to predict the effective temperature in the gaseous region are shown below:

$$\frac{T_R - T_{eff}}{T_R - T_v} = e^{-\left[\frac{h_{cg} A}{\phi C_{p_g} W_{fc}}\right]}$$

and
$$\frac{1}{\phi} = \left(\frac{S V_g}{\alpha_c}\right)^{1/8} f\left(\frac{V_g}{V_c}\right)$$

For:
$$\frac{V_g}{V_c} \leq 1.0, \quad f\left(\frac{V_g}{V_c}\right) = \left(\frac{V_c}{V_g}\right)^{1.5} \left(\frac{V_c}{V_g} - 1\right)$$

For:
$$\frac{V_g}{V_c} > 1.0, \quad f\left(\frac{V_g}{V_c}\right) = 1 + 0.4 \tan^{-1} \left(\frac{V_g}{V_c} - 1\right)$$

Where:

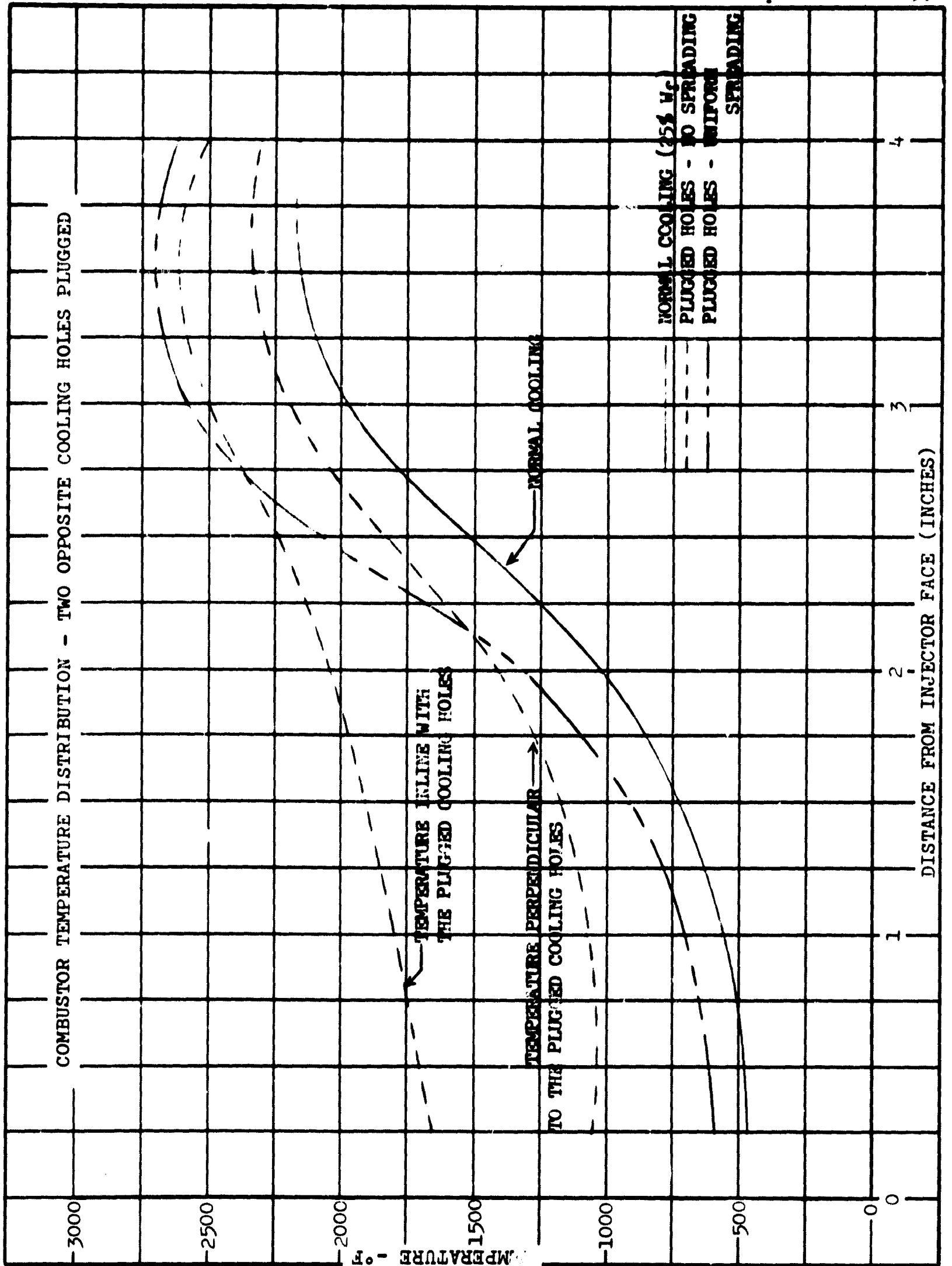
- A = Internal chamber surface area
- S = Film height
- V = velocity
- α = thermal diffusivity
- ϕ = efficiency factor
- C_{p_g} = constant pressure specific heat for a gas

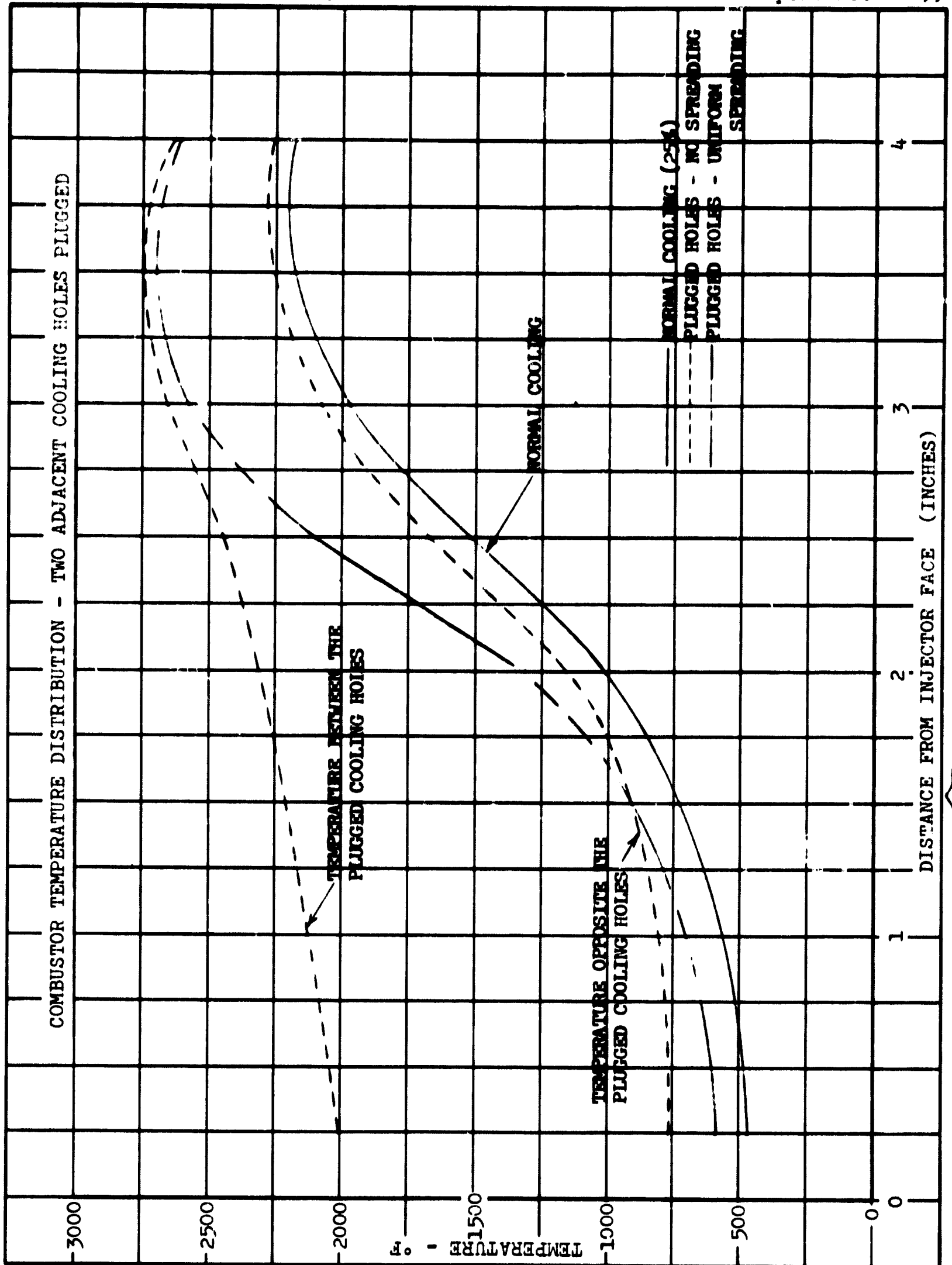
Subscripts:

- v = vapor
- g = gas
- c = coolant
- eff = effective

These equations were programmed for the IBM 360/40 to predict effective gas temperatures at various distances from the injector face.

Since it is not known just how the cooling flow from the unplugged holes will spread out on the chamber walls, two models were assumed, one with uniform spreading to the area downstream of the plugged cooling holes and the other with no spreading. The actual phenomenon lies somewhere between these extremes. For the spreading case, it was assumed that the chamber is cooled by a uniformly distributed cooling flow which is 75% of nominal (to account for the plugged holes). For the no spreading case it was assumed that each cooling hole cools one eighth of the combustor wall and that the wall downstream of the plugged hole sees the full main core combustion temperature. These hotter areas are assumed to be cooled by conduction to other parts of the chamber and by radiation to space, but not by flow from adjacent film cooling holes. To achieve maximum accuracy in these calculations, the thermal conductivity of molybdenum was input as a function of temperature. The results of this analysis is shown on Figures 6, 7, and 8.





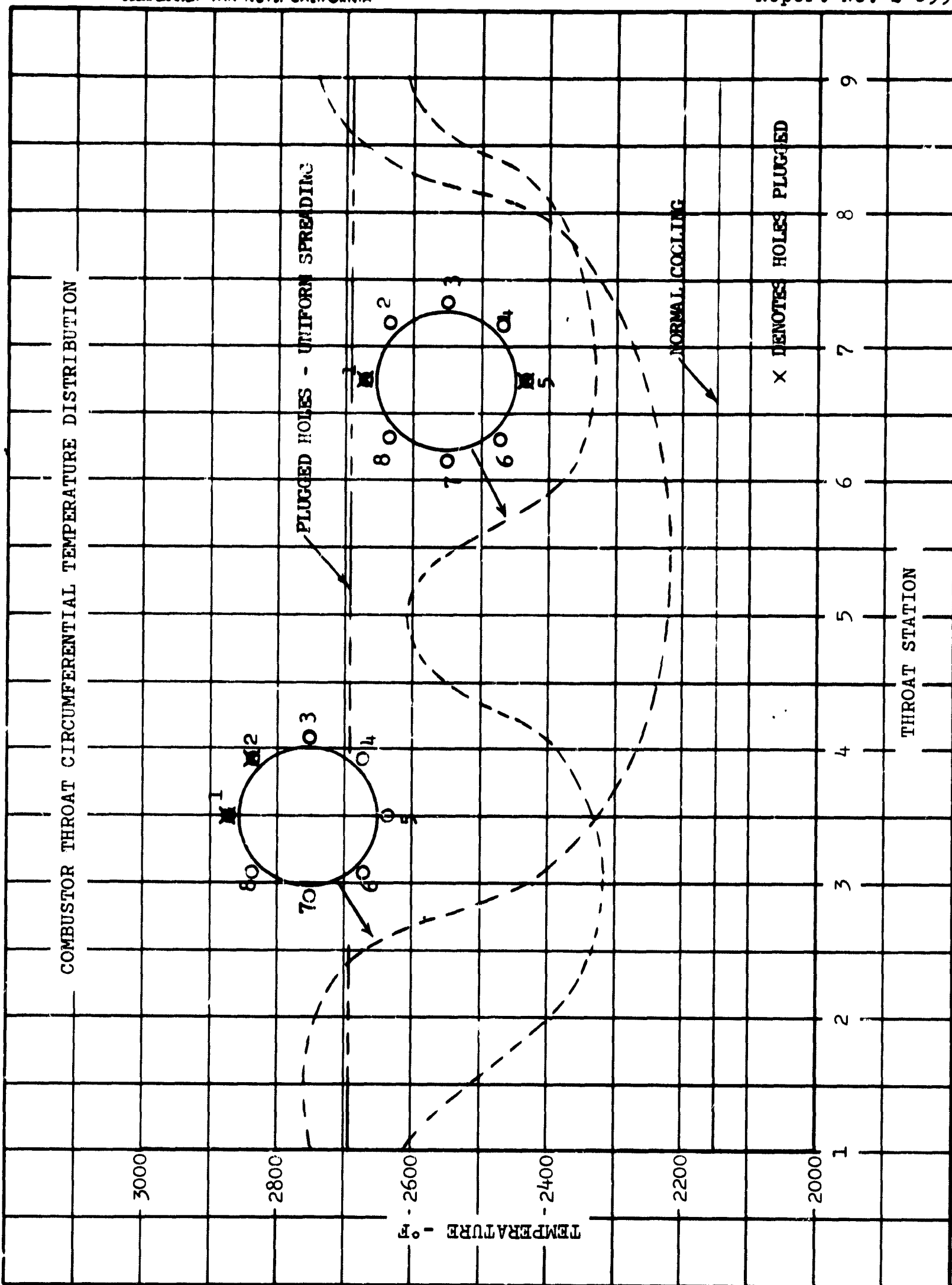


Figure 6 shows the combustor temperature as a function of distance from the injector face when two opposite cooling holes are plugged. The results are shown for the two coolant spreading assumptions and for a nominal (unplugged cooling holes) R-4D engine. For the no spreading case the temperatures in the plane of the plugged holes and the temperatures along the combustor in a plane perpendicular to the plane formed by the plugged holes are shown. These represent the maximum and minimum combustor temperatures for this case. None of the temperatures predicted here should cause any problems even for extended operation since the R-4D combustor has withstood similar temperatures for times far in excess of 50 seconds.

Figure 7 is the same as Figure 6 except that it is representative of two adjacent holes being plugged. Analysis results indicate that the chamber wall will reach a maximum temperature of 2750°F with no spreading of the cooling flow. As mentioned earlier, the no spreading case is probably unrealistic, however, if temperatures did reach this level the combustor would be adequate for several hours of engine operation.

Figure 8 shows the results for both the opposite plugged cooling holes and the adjacent plugged holes at the throat location showing the angular variation.

It should be noted that this analysis does not adequately predict chamber wall temperatures close to the injector face. Core gas temperatures close to the injector depend upon reaction kinetics and also upon the particular injector geometry. For these reasons one would expect that the chamber flange temperatures for the non-spreading case are actually lower than indicated in Figures 6 and 7.

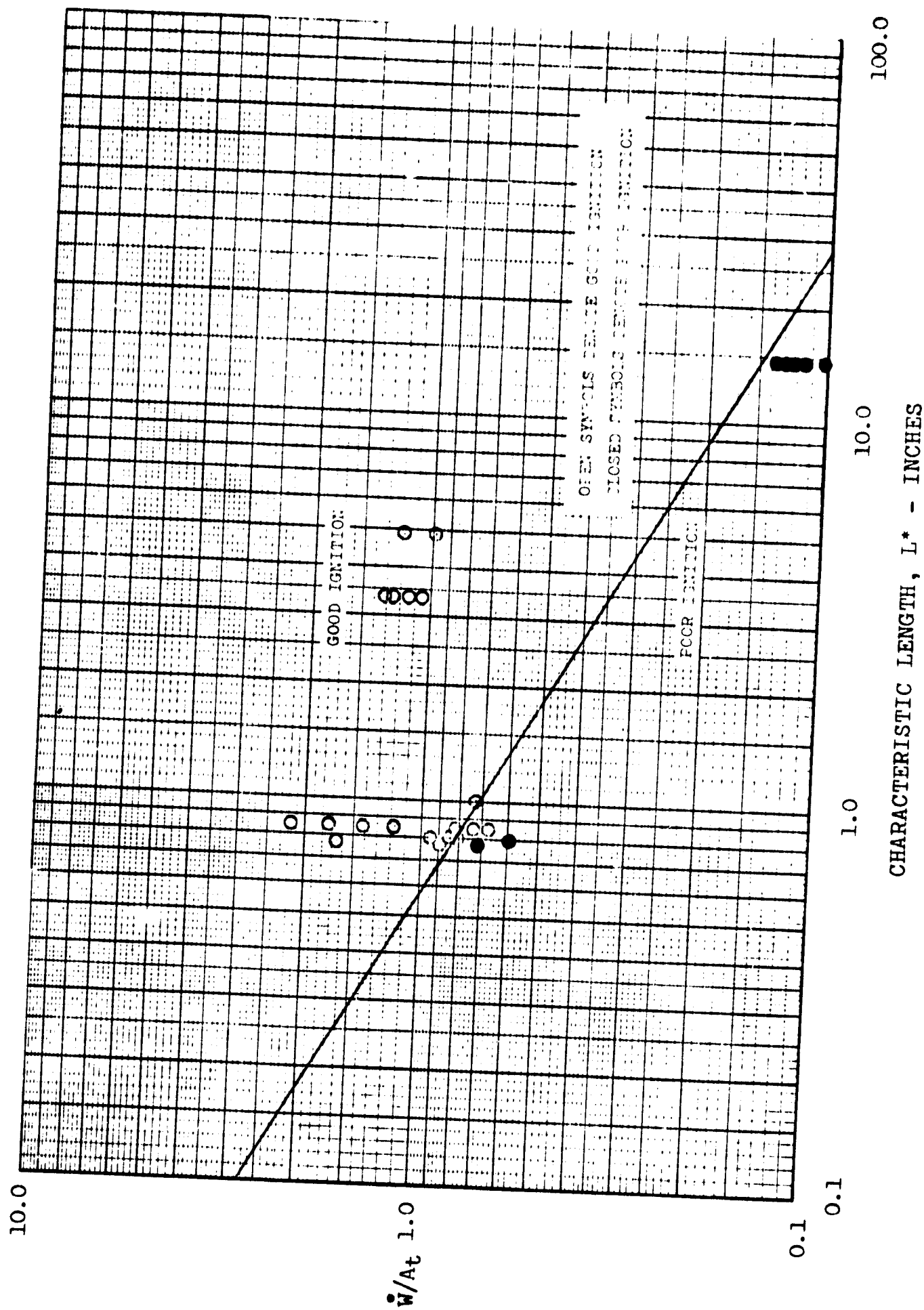
C. Ignition at Off-Limits Conditions

The R-4D engine utilizes a preigniter chamber to ensure engine structural integrity during engine ignition over the range of expected operating conditions. The ignition tests simulating clogged propellant filters present extreme conditions for engine ignition since the flow rate to the preigniter (and the main doublet) is throttled, thereby reducing the effectiveness of the preigniter. Engine operation at these test conditions was analyzed to predict whether or not potentially damaging ignition might result during the Severe Off-Limits tests.

Previous development test experience has shown for normal valve mismatches (i.e., application of voltage simultaneously to both valves) at or near design operating conditions, that long ignition delays (defined as time from last propellant valve open to ignition) always accompany ignition overpressures of magnitudes great enough to cause engine damage. Therefore, the test conditions of the simulated clogged filter tests were studied to predict if consistent rapid ignition could be expected or if long ignition delays could occur. The conditions where inconsistent or long ignition delays could occur would be considered hazardous since potentially damaging ignition overpressures are possible.

Data previously generated with an Apollo RCS development engine provides relationships between engine design parameters and satisfactory ignition. Satisfactory ignition is defined as consistently low ignition delays. The development engine incorporated a four valve arrangement where one pair of valves fed the eight main chamber doublets and the other pair fed a single doublet located in the center of the injector. Replaceable preigniter chambers of various shapes could be attached around the center doublet by means of four tapped holes in the injector. Tests were run with various preigniter cup configurations and flow rates from the center doublet to evaluate the effects of small L^* 's, throat areas and flow rates upon ignition. Also, the preigniter cup was removed and tests conducted using the eight outer doublets with several main combustor configurations to evaluate larger L^* chambers. The results of these tests are shown in Figure 9 where satisfactory engine ignition is shown to be a function of L^* , propellant flow rate, and combustor throat area. The open symbols denote conditions where satisfactory ignition was experienced and the solid symbols denote conditions where excessive ignition delays or no ignition at all occurred. The line provides an approximate boundary between regions of good and poor ignition. The test results locate the position of line at an L^* of about .8 inches but not at larger or smaller L^* 's. Analysis results contained in Reference 2 indicate that the slope of the line on Figure 9 should be about -1. The test results at L^* of 14 inches force the slope to be a little less if the line is assumed to lie just above the "poor ignition" data points. Any test condition falling into the region below the line on Figure 9 may result in excessive ignition delays and large ignition overpressures while those conditions in the region above the line should result in satisfactory engine ignition.

IGNITION LIMITS



The ignition criteria discussed above were applied to the tests to be conducted at conditions simulating clogged propellant filters. Two preignition situations were considered for each of the ignition test conditions specified in Table I. The first consideration was whether good ignition would occur in the preigniter and the second was whether ignition would result in the main combustor should the preigniter not light. The main chamber ignition case was analyzed to determine if impulse would be delivered by the engine should ignition not occur in the preigniter.

The propellant flow rates into the preigniter prior to filling the manifold dribble volumes and the flow rates into the main chamber should the preigniter not light were calculated at the off-design conditions using an injector hydraulics computer program. The calculated total flow rates, O/F and \dot{w}/A_t , during start up for the two flow situations considered are tabulated in Table VII. The values of \dot{w}/A_t for both situations are plotted versus the appropriate chamber L^* on Figure 10.

Figure 10 indicates that poor ignition will result for the preigniter situation for two of the test conditions. These conditions are those with the lowest oxidizer inlet pressures which was to be expected since due to the injector design the oxidizer provides the bulk of the total flow to the preigniter. Two other conditions - those at the next lowest oxidizer inlet pressures of 100 psia - are marginal.

Ignition may occur in the preigniter after the dribble volume is filled since the flow rate to the preigniter increases (by about 10%) due to the increased fluid pressure just downstream of the valve. This case does not fit the "satisfactory ignition" definition due to the time delay and therefore an analysis for this case was not considered.

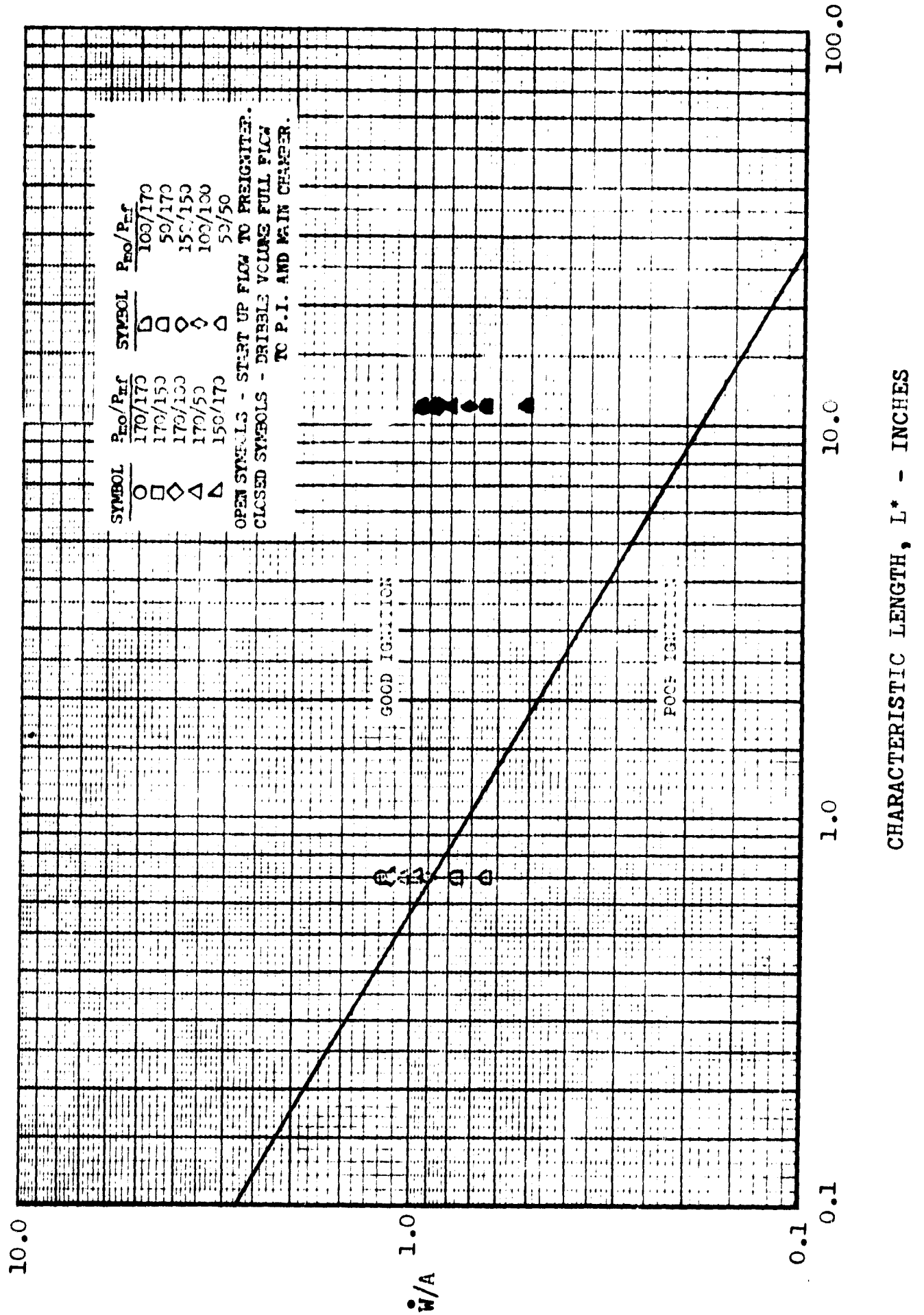
START UP FLOW FOR R-4D ENGINE AT SIMULATED CLOGGED FILTER CONDITIONS

Fuel Inlet Pressure (Psia)	Ox Inlet Pressure (Psia)	Preigniter Flow Prior to Dribble Volume Filling		Total Flow Into Main Chamber When Dribble Volume Full	
		O/F	\dot{W} (Lb./sec)	O/F	Lb./sec
170	170	3.28	.1128	2.05	.5535
150	170	3.49	.1112	2.19	.5426
100	170	4.27	.167	2.68	.5112
50	170	6.04	.1007	3.79	.4706
170	150	3.08	.1076	1.93	.5310
170	100	2.51	.0927	1.58	.4663
170	50	1.78	.0733	1.11	.3832
150	150	3.28	.1059	2.05	.5200
100	100	3.28	.0865	2.05	.4246
50	50	3.28	.0612	2.05	.3002

Preigniter L* = .693 inches
 Main Chamber L* = 11.2 inches
 Preigniter A_t = .09611 in²
 Main Chamber A_t = .5914 in²

Propellants N₂O₄/MMH
 Orificed for O/F = 2.03
 F = 100#

SEVERE OFF LIMITS IGNITION



IV. CONCLUSIONS & RECOMMENDATIONS

The analysis of the steady state tests simulating SM-LM RCS engine operation with partially clogged propellant line filters indicate that the preigniter will probably burn out during one of the planned runs. The expected burnout should occur on either the fifty second run conducted with equal oxidizer and fuel inlet supply pressures of 100 psia, or the fifty second run with 50 psia inlet pressures. The test plan (Reference 1) specifies that the 50 psia condition will not be tested should engine damage occur during testing at the 100 psia condition, thus only one burnout is expected. The preigniter burnout would result from insufficient fuel film cooling of the tip of the preigniter cup.

Inconsistent and delayed preigniter operation is predicted for both of the ignition tests with the 50 psia oxidizer inlet pressures (conditions 2-C and 3-C of Table I). The erratic preigniter operation is due to insufficient propellant mass flow into the preigniter. The resulting long ignition delays may lead to excessive ignition overpressures and engine combustor damage.

Engine damage during the simulated regulator failure test run is probable. The failure mode, should this occur, would be preigniter burnout resulting from insufficient fuel film cooling of the preigniter.

The analysis of the tests with two engine configurations with plugged holes predicts that neither test is severe enough to expect engine damage. Other configurations should be considered where the #1 preigniter cooling hole is partially plugged or those holes adjacent to this hole be plugged.

It is recommended that the Severe Off-Limits tests be conducted in the order specified in Reference 1 (MTP 0080) without alteration. The tests at conditions of expected or probable engine damage are separated by sufficient time to make the needed engine repairs prior to encountering the next potentially damaging test run.

APPENDIX A

OFF DESIGN STEADY STATE AND PULSE PERFORMANCE

PROGRAM

This Quiktran computer program computes steady state or pulse performance at off design conditions.

The computer program was written so that the computer requests the input information.

Tables A-I and A-II are examples of the pulse and steady state output. The program has two performance curves built into it. Propellant Code 0 results in the use of the curve for the propellant combination of Aerozine-50 and N_2O_4 ; Propellant Code 1 results in the use of MMH- N_2O_4 performance curve.

Table A-III is the listing for the program.

APPENDIX A

TABLE A-1

COMPUTER OUTPUT-PULSE

103.	=0	08	INPUT INITIAL F, PC, O/F, ISP, PTANK, PROPELLANT CODE
105.	=1	00	100./97./2.03/280.5/170./1
106.	=0	07	INPUT CALCULATION MODE (0=STEADY STATE, 1=PULSES)
108.	=1	00	1
153.	=0	09	INPUT TO, TF, PO, PF
155.	=1	00	75./75./170./170.
199.	=0	43	INPUT PULSE WIDTH (MS) AND KEY
201.	=1	00	20./1
208.	=0	44	PULSE O/F= 1.7600 PULSE ISP= 188.568
199.	=0	43	INPUT PULSE WIDTH (MS) AND KEY
201.	=1	00	50./1
208.	=0	44	PULSE O/F= 1.9445 PULSE ISP= 236.695
199.	=0	43	INPUT PULSE WIDTH (MS) AND KEY
201.	=1	00	100./1
208.	=0	44	PULSE O/F= 1.9909 PULSE ISP= 258.000
199.	=0	43	INPUT PULSE WIDTH (MS) AND KEY
201.	=1	00	500./0
208.	=0	44	PULSE O/F= 2.0228 PULSE ISP= 276.596
153.	=0	09	INPUT TO, TF, PO, PF
155.	=1	00	75./75./170./150.
199.	=0	43	INPUT PULSE WIDTH (MS) AND KEY
201.	=1	00	20./1
208.	=0	44	PULSE O/F= 2.0106 PULSE ISP= 180.734
199.	=0	43	INPUT PULSE WIDTH (MS) AND KEY
201.	=1	00	50./1
208.	=0	44	PULSE O/F= 2.2410 PULSE ISP= 226.285
199.	=0	43	INPUT PULSE WIDTH (MS) AND KEY
201.	=1	00	100./1
208.	=0	44	PULSE O/F= 2.3013 PULSE ISP= 247.307
199.	=0	43	INPUT PULSE WIDTH (MS) AND KEY
201.	=1	00	500./0
208.	=0	44	PULSE O/F= 2.3436 PULSE ISP= 265.132
153.	=0	09	INPUT TO, TF, PO, PF
155.	=1	00	75./75./170./100.
199.	=0	43	INPUT PULSE WIDTH (MS) AND KEY
201.	=1	00	20./1
208.	=0	44	PULSE O/F= 3.1619 PULSE ISP= 145.091
199.	=0	43	INPUT PULSE WIDTH (MS) AND KEY
201.	=1	00	50./1
208.	=0	44	PULSE O/F= 3.6000 PULSE ISP= 182.140
199.	=0	43	INPUT PULSE WIDTH (MS) AND KEY
201.	=1	00	100./1
208.	=0	44	PULSE O/F= 3.7237 PULSE ISP= 198.535
199.	=0	43	INPUT PULSE WIDTH (MS) AND KEY
201.	=1	00	500./0
208.	=0	44	PULSE O/F= 3.8142 PULSE ISP= 212.844

153.	=0	09	INPUT TO, TF, PO, PF	
155.	=1	00	75./75./170./50.	
199.	=0	43	INPUT PULSE WIDTH (MS) AND KEY	
201.	=1	00	20./1	
208.	=0	44	PULSE O/F= 5.4618 PULSE ISP=	72.588
199.	=0	43	INPUT PULSE WIDTH (MS) AND KEY	
201.	=1	00	50./1	
208.	=0	44	PULSE O/F= 6.3461 PULSE ISP=	91.123
199.	=0	43	INPUT PULSE WIDTH (MS) AND KEY	
201.	=1	00	100./1	
208.	=0	44	PULSE O/F= 6.6105 PULSE ISP=	99.325
199.	=0	43	INPUT PULSE WIDTH (MS) AND KEY	
201.	=1	00	500./0	
208.	=0	44	PULSE O/F= 6.8103 PULSE ISP=	106.485
153.	=0	09	INPUT TO, TF, PO, PF	
155.	=1	00	75./75./150./170.	
199.	=0	43	INPUT PULSE WIDTH (MS) AND KEY	
201.	=1	00	20./1	
208.	=0	44	PULSE O/F= 1.5463 PULSE ISP=	194.90?
199.	=0	43	INPUT PULSE WIDTH (MS) AND KEY	
201.	=1	00	50./1	
208.	=0	44	PULSE O/F= 1.6852 PULSE ISP=	244.671
199.	=0	43	INPUT PULSE WIDTH (MS) AND KEY	
201.	=1	00	100./1	
208.	=0	44	PULSE O/F= 1.7187 PULSE ISP=	266.694
199.	=0	43	INPUT PULSE WIDTH (MS) AND KEY	
201.	=1	00	500./0	
208.	=0	44	PULSE O/F= 1.7409 PULSE ISP=	285.917
153.	=0	09	INPUT TO, TF, PO, PF	
155.	=1	00	75./75./100./170.	
199.	=0	43	INPUT PULSE WIDTH (MS) AND KEY	
201.	=1	00	20./1	
208.	=0	44	PULSE O/F= 0.9886 PULSE ISP=	183.628
199.	=0	43	INPUT PULSE WIDTH (MS) AND KEY	
201.	=1	00	50./1	
208.	=0	44	PULSE O/F= 1.0430 PULSE ISP=	230.518
199.	=0	43	INPUT PULSE WIDTH (MS) AND KEY	
201.	=1	00	100./1	
208.	=0	44	PULSE O/F= 1.0535 PULSE ISP=	251.267
199.	=0	43	INPUT PULSE WIDTH (MS) AND KEY	
201.	=1	00	500./0	
208.	=0	44	PULSE O/F= 1.0591 PULSE ISP=	269.378

153.	=0	09	INPUT TO, TF, PO, PF	
155.	=1	00	75./75./ 50./170.	
199.	=0	43	INPUT PULSE WIDTH (MS) AND KEY	
201.	=1	00	20./1	
208.	=0	44	PULSE O/F= 0.5259 PULSE ISP=	118.100
199.	=0	43	INPUT PULSE WIDTH (MS) AND KEY	
201.	=1	00	50./1	
208.	=0	44	PULSE O/F= 0.5383 PULSE ISP=	148.257
199.	=0	43	INPUT PULSE WIDTH (MS) AND KEY	
201.	=1	00	100./1	
208.	=0	44	PULSE O/F= 0.5386 PULSE ISP=	161.602
199.	=0	43	INPUT PULSE WIDTH (MS) AND KEY	
201.	=1	00	500./0	
208.	=0	44	PULSE O/F= 0.5374 PULSE ISP=	173.250
153.	=0	09	INPUT TO, TF, PO, PF	
155.	=1	00	75./75./ 150./150.	
199.	=0	43	INPUT PULSE WIDTH (MS) AND KEY	
201.	=1	00	20./1	
208.	=0	44	PULSE O/F= 1.7718 PULSE ISP=	188.214
199.	=0	43	INPUT PULSE WIDTH (MS) AND KEY	
201.	=1	00	50./1	
208.	=0	44	PULSE O/F= 1.9481 PULSE ISP=	236.276
199.	=0	43	INPUT PULSE WIDTH (MS) AND KEY	
201.	=1	00	100./1	
208.	=0	44	PULSE O/F= 1.9926 PULSE ISP=	257.543
199.	=0	43	INPUT PULSE WIDTH (MS) AND KEY	
201.	=1	00	500./0	
208.	=0	44	PULSE O/F= 2.0231 PULSE ISP=	276.106
153.	=0	09	INPUT TO, TF, PO, PF	
155.	=1	00	75./75./100./100.	
199.	=0	43	INPUT PULSE WIDTH (MS) AND KEY	
201.	=1	00	20./1	
208.	=0	44	PULSE O/F= 1.8000 PULSE ISP=	187.293
199.	=0	43	INPUT PULSE WIDTH (MS) AND KEY	
201.	=1	00	50./1	
208.	=0	44	PULSE O/F= 1.9571 PULSE ISP=	235.119
199.	=0	43	INPUT PULSE WIDTH (MS) AND KEY	
201.	=1	00	100./1	
208.	=0	44	PULSE O/F= 1.9968 PULSE ISP=	256.282
199.	=0	43	INPUT PULSE WIDTH (MS) AND KEY	
201.	=1	00	500./0	
208.	=0	44	PULSE O/F= 2.0239 PULSE ISP=	274.755

153.	=0 09	INPUT TO TE. PULPE	
155.	=1 00	75./75./50./50.	
199.	=0 43	INPUT PULSE WIDTH (MS) AND KEY	
201.	=1 00	20./1	
208.	=0 44	PULSE O/F= 1.8262 PULSE ISP=	186.182
199.	=0 43	INPUT PULSE WIDTH (MS) AND KEY	
201.	=1 00	50./1	
208.	=0 44	PULSE O/F= 1.9658 PULSE ISP=	233.724
199.	=0 43	INPUT PULSE WIDTH (MS) AND KEY	
201.	=1 00	100./1	
208.	=0 44	PULSE O/F= 2.0010 PULSE ISP=	254.761
199.	=0 43	INPUT PULSE WIDTH (MS) AND KEY	
201.	=1 00	500./0	
208.	=0 44	PULSE O/F= 2.0247 PULSE ISP=	273.124

APPENDIX A
TABLE A-II
COMPUTER OUTPUT-STEADY STATE

103.	=0	08	INPUT NOMINAL F, PC, O/F, ISP, PTANK, PROPELLANT CODE				
105.	=1	00	100./96.5/2.03/281.5/170./1				
149.	=0	09	INPUT TO, TF, PO, PF				
151.	=1	00	75./75./170./170.				
183.	=0	04	O/F=	F=	ISP=	PC=	96.500
149.	=0	09	INPUT TO, TF, PO, PF				
151.	=1	00	75./75./170./150.				
183.	=0	04	O/F=	F=	ISP=	PC=	91.393
<hr/>							
149.	=0	09	INPUT TO, TF, PO, PF				
151.	=1	00	75./75./170./100.				
183.	=0	04	O/F=	F=	ISP=	PC=	72.513
149.	=0	09	INPUT TO, TF, PO, PF				
151.	=1	00	75./75./170./50.				
183.	=0	04	O/F=	F=	ISP=	PC=	38.456
149.	=0	09	INPUT TO, TF, PO, PF				
151.	=1	00	75./75./150./170.				
183.	=0	04	O/F=	F=	ISP=	PC=	92.724
149.	=0	09	INPUT TO, TF, PO, PF				
151.	=1	00	75./75./100./170.				
183.	=0	04	O/F=	F=	ISP=	PC=	73.479
149.	=0	09	INPUT TO, TF, PO, PF				
151.	=1	00	75./75./ 50./170.				
183.	=0	04	O/F=	F=	ISP=	PC=	40.902
149.	=0	09	INPUT TO, TF, PO, PF				
151.	=1	00	75./75./ 150./150.				
183.	=0	04	O/F=	F=	ISP=	PC=	88.276
149.	=0	09	INPUT TO, TF, PO, PF				
151.	=1	00	75./75./100./100.				
183.	=0	04	O/F=	F=	ISP=	PC=	65.592
149.	=0	09	INPUT TO, TF, PO, PF				
151.	=1	00	75./75./ 50./ 50.				
183.	=0	04	O/F=	F=	ISP=	PC=	38.195

TABLE A-III
PROGRAM LISTING

```

101. = CF PROGRAM PIPERF
102. = C ROCKET ENGINE PERFORMANCE CALCULATION - K KERSO' EXT 1257
103. = PRINT 8
104. = 8 FORMAT(49H INPUT NOMINAL F, PC, O/F, ISP, PTANK, PROPELLANT CODE)
105. = CF READ O, F, PC, RMIX, ATSP, PROT, J
106. = PRINT 7
107. = 7 FORMAT(49H INPUT CALCULATION MODE (0=STEADY STATE, 1=PULSES))
108. = CF READ O, ICODE
109. = WF=F/(ATSP*(1.+RMIX))
110. = W0=RMIX*WF
111. = TCO=PC/F
112. = XK0=VK/SQRT(PNOM-PC)
113. = XKF=WF/SQRT(PNOM-PC)
114. = IF(J-1)20, 30, 40
115. = C THIS SECTION SETS ISP CONSTANTS FOR A-50, N204 COMBINATION
116. = 20 B2=-1.74448E-1
117. = B3=5.33063E-4
118. = B4=-2.20301E1
119. = B5=-7.77798
120. = A2=B2
121. = A3=B3
122. = A4=2.65989E2
123. = A5=-1.40401E2
124. = A6=2.02659E1
125. = A7=6.0E-2
126. = A8=1.14710E-1
127. = GO TO 31
128. = C THIS SECTION FIXES ISP CONSTANTS FOR MM1, N204 COMBINATION
129. = 30 B2=-1.74448E-1
130. = B3=5.33063E-4
131. = B4=-43.6032
132. = B5=0.
133. = A2=B2
134. = A7=B3
135. = A4=5.50087E2
136. = A5=-2.96451E2
137. = A6=4.91304E1
138. = A7=6.0E-2
139. = A8=1.14710E-1
140. = 31 T=75.
141. = IF(RMIX=2.)21, 22, 22
142. = 21 A1=ATSP-A2*T-A3*T**2-A4*RMIX-A5*RMIX**2-A6*RMIX**3-A7*PC-A8*T*RMIX
143. = RMIX=2.
144. = XISP=A1+A2*T+A3*T**2+A4*RMIX+A5*RMIX**2+A6*RMIX**3+A7*PC+A8*T*RMIX
145. = B1=XISP-B2*T-B3*T**2-B4*RMIX-B5*RMIX**2-A7*PC-A8*T*RMIX
146. = GO TO 3
147. = 22 B1=ATSP-B2*T-B3*T**2-B4*RMIX-B5*RMIX**2-A7*PC-A8*T*RMIX
148. = RMIX=2.

```

```

149. = XI SP = B1 + B2 * T + B3 * T ** 2 + B4 * RMIX + B5 * RMIX ** 2 + A7 * PC + A8 * T * RMIX
150. = RMIX = RMIX
151. = A1 = XI SP - A2 * T - A3 * T ** 2 - A4 * RMIX - A5 * RMIX ** 2 - A6 * RMIX ** 3 - A7 * PC - A8 * T * RMIX
152. = 3 CONTINUE
153. = PRINT 9
154. = 9 FORMAT(18H INPUT TO, TF, P(), PF)
155. = CF READ 0, TO, TF, PO, PF
156. = F = 100.
157. = K = 0
158. = N = 0
159. = 5 IF(K-1)11, 18, 3
160. = 18 N = N + 1
161. = IF(N-1)17, 17, 81
162. = 81 F = F2 + (F - F2) * .2
163. = 17 F2 = F
164. = 11 PC = F * TCO
165. = IF(PC - PC)12, 12, 13
166. = 12 K = K + 1
167. = F = F - 10.
168. = GO TO 5
169. = 13 IF(PF - PC)14, 14, 15
170. = 14 K = K + 1
171. = F = PF - 10.
172. = GO TO 5
173. = 15 CONTINUE
174. = V() = XK() * SQRT(PC - PC)
175. = V F = XKF * SQRT(PF - PC)
176. = RMIX = V() / V F
177. = T = (TO + TF) / 2.
178. = IF(RMIX - 2.)70, 71, 71
179. = 70 XI SP = A1 + A2 * T + A3 * T ** 2 + A4 * RMIX + A5 * RMIX ** 2 + A6 * RMIX ** 3 + A7 * PC + A8 * T * RMIX
180. = GO TO 72
181. = 71 XI SP = B1 + B2 * T + B3 * T ** 2 + B4 * RMIX + B5 * RMIX ** 2 + A7 * PC + A8 * T * RMIX
182. = 72 F1 = XI SP * (V() + V F)
183. = IF(ABS(F1 - F) - .001)2, 2, 1
184. = 1 F = F1
185. = GO TO 5
186. = 2 IF(NODE)41, 41, 42
187. = 41 CONTINUE
188. = PRINT 4, RMIX, F, XI SP, PC
189. = 4 FORMAT(5H O/F =, F8.4, 5H F =, F10.3, 7H ISP =, F10.3, 6H PC =, F10.3)

```

```

190. = GO TO 3
191. = 42 AB1=9.084649E-2
192. = AB2=-4.21606E-3
193. = AB3=-2.06744
194. = AB4=0.453602
195. = BB1=6.31497E-3
196. = BB2=-9.578E-5
197. = BB3=-3.318768
198. = BB4=.8994022
199. = PRINT 43
200. = 43 FORMAT(5H INPUT PULSE WIDTH (MS) AND KEY)
201. = CF READ 0, EPI, KEY
202. = R=PIIX*(EPI-1.85E-2*PI)+1.15-17.67/EPI/(EPI-1.46E-2*PI+2.23)
203. = IF (EPI-100.)45,46,46
204. = 45 XISP2=(AB1*SQRT(EPI)+AB2*PI+AB3/EPI+AB4)*XISP
205. = GO TO 47
206. = 46 XISP2=(BB1*SQRT(EPI)+BB2*PI+BB3/EPI+BB4)*XISP
207. = 47 CONTINUE

```

```

208. = PRINT 44, R, XISP2
209. = 44 FORMAT(11H PULSE O/F=,F8.4,11H PULSE ISP=,F10.3)
210. = IF (KEY)3,3,42
211. = END

```